Aalborg Universitet

AALBORG UNIVERSITY
DENMARK

Linear Active Disturbance Rejection Control for LCL Type Grid-connected Converter

Lu, Jinghang; Savaghebi, Mehdi; Guerrero, Josep M.; Quintero, Juan Carlos Vasquez; Xie, Chuan

Linear Active Disturbance Rejection Control for LCL Type Grid-connected Converter

Jinghang Lu, Mehdi Savaghebi, Josep M.Guerrero,
Juan C.Vasquez

Department of Energy Technology
Aalborg University, Denmark

{jgl,mes,juq,joz}@et.aau.dk

Chuan Xie

School of Automation Engineering
Univ. of Electronic Sci&Tech of China
Chengdu, China
c.xie@uestc.edu.cn

Abstract—**This paper presents a linear active disturbance rejection control (LADRC) for grid-connected converter with LCL filter. The high rejection performance for external disturbance, internal decoupling, parameter variation is achieved by adopting extended state observer(ESO) and designing controller with direct pole placement. Robustness of parameter uncertainty and sensitivity of input disturbance are analyzed in frequency domain to demonstrate the superior characteristic in disturbance rejection. The theoretical analysis is verified in Matlab/Simulink. The simulation results show the excellent capability of rejection in grid voltage disturbance.**

Keywords—LADRC; Extended State Observer; LCL filter;

I. INTRODUCTION

With the scarcity of fossil fuels and public's attention diverting into renewable energy based Distributed Generation(DG) system, the power conversion unit as the main part of DG system is drawing increasing attention [1]. Grid-connected inverter as an energy conversion interface plays a crucial role in delivering high quality power into the grid. To reduce the switching ripple and improve quality of grid current, LCL filters are usually adopted as interface between inverter and utility as LCL filter can offer better high-order harmonic attenuation, lower voltage drops over inductance and reduced physical size comparing with L type filter [2].

Meanwhile, the resonance of LCL filter that is the main drawback has been broadly investigated and discussed by adopting passive damping or virtual impedance based active damping methods [3]. On the other hand, state-space control offers an alternative way to straightforwardly achieve resonance damping and fast dynamic response by directly placing the closed-loop poles to the desired position [4].

In state-space control methods, various methods have been analyzed such as deadbeat control, linear quadratic control(LQC). However, the deadbeat control is quite sensitive to parameter variation while cost function of LQC is difficult to select [5]. On the contrary, by adopting direct pole placement method, analysis can be performed by tool of classical control methods such as: bode plot and root loci, which is intuitive for implementation [6].

In addition, with more stringent international standard and grid code for DG system, grid-connecting inverters are required to have the ability of voltage disturbance rejection, which indicates grid-connecting inverter is able to deliver balanced sinusoidal waveform with low harmonic content at the point of common coupling(PCC) and perform excellent voltage disturbance rejection capability.

To achieve the aforementioned goal, various approaches have been widely studied, in [7] an observer based voltage feed-forward control strategy is added to the fundamental control scheme. In [6] an extended state observer is utilized for the voltage disturbance rejection where the low harmonic voltage is modeled as extended state. However, this method can only deal with external disturbance while internal dynamic variation that affects the stable operation of the system as well can not be handled by the aforementioned method.

On the other hand, active disturbance rejection control (ADRC) [8] is emerging as an alternative to deal with the total disturbance and has been successfully adopted in motor drive system, power system and active power filter (APF) control. In contrast to model each disturbance in the system as the extended state, ADRC consider the total disturbance-both the external disturbance and internal dynamic variation as one state that is estimated and compensated in real time by utilizing extended state observer (ESO) [9]. Therefore, on the contrary to the conventional state observer and disturbance observer (DOB) [10], ADRC do not rely on accurate mathematical model of the plant, hence, it is very robust to parameter variation, noise and disturbance. However, heavy computation burden and large number of parameter of ADRC to be tuned impede wide application in the industry. In this paper, a modified linear ADRC [9] (LADRC) is proposed for LCL type grid-connecting converter, where external disturbance and internal dynamics rejection are achieved Moreover, the controller is designed to achieve zero steady state error based on system closed-loop bandwidth and relationship with observer's bandwidth, Frequency domain analysis is conducted to demonstrate the robustness of LADRC to total disturbance.

The rest of the paper is organized as following. Section II presents the linear LADRC structure for LCL filter. Section III provides comprehensive frequency analysis of the ADRC based control system. Section IV provides the case study by simulation to demonstrate the effectiveness of the proposed control strategy. The conclusion of the paper is drawn in Section V.

II. LADRC DEISGN

Conventional observer based control strategy design inevitably needs to describe accurate mathematical model of the plant where internal dynamic and parameter of the system are actually unavailable in real world. The ADRC that was proposed by Han [8], departing from the existing model-based paradigm, can estimate state including the total disturbance without an accurate mathematical model. Its core idea is to consider the total disturbance (external disturbance and internal dynamics) as an extended state that will be observed and compensated by properly designing the observer. Therefore, ideally, the disturbance will not have effect on the system output.
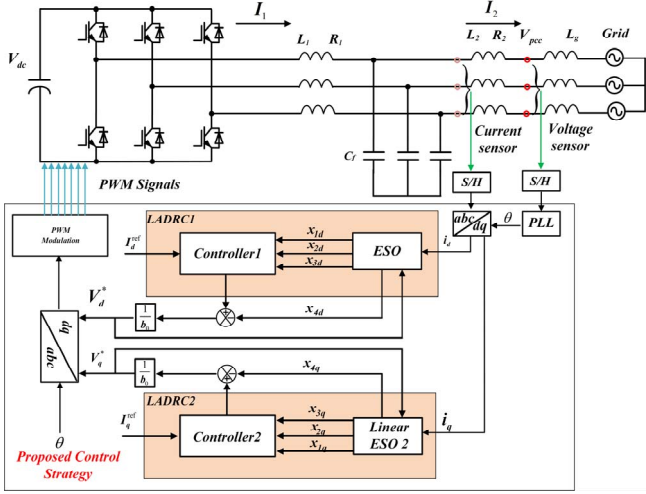

Fig. 1.   Diagram of grid-connected converter with LADRC strategy

A. LESO design

Fig.1 describes the power stage of LCL type filter with proposed control strategies, where three phase grid-connected inverter with LCL filters is interfacing into the grid through a line impedance. The LCL filter consists of a converter side inductor L_1, filter capacitor C_f, a grid side inductor L_2, L_g is the grid impedance. In this paper the grid side inductor current is controlled to achieve unit power factor at the PCC. Complex space vectors in synchronous dq frame are implemented ($i_2 = i_{2d} + ji_{2q}$). Therefore, the state-space model of LCL type grid-connecting inverter in a rotating reference frame [5] is expressed as:

$$\dot{x} = \begin{bmatrix} -jw_g & \frac{1}{L_2} & 0 \\ \frac{1}{C_f} & -jw_g & -\frac{1}{C_f} \\ 0 & -\frac{1}{L_1} & -jw_g \end{bmatrix} x + \begin{bmatrix} 0 \\ 0 \\ \frac{1}{L_1} \end{bmatrix} V_t + \begin{bmatrix} -\frac{1}{L_2} \\ 0 \\ 0 \end{bmatrix} V_{pcc}$$

$$i_2 = [1 \quad 0 \quad 0]x \tag{1}$$

Where $x = [i_2, v_c, i_1]^T$, i_2 is the grid side inductor current, v_c is the capacitor voltage, i_1 is the converter side inductor current, V_t is the converter output voltage, V_{pcc} is the PCC voltage. In the synchronous coordinate rotating frame, w_g is the grid angular frequency, parasitic element of the filter components is

neglected to design the worse-case situation of resonance LCL filter.

The transfer function from inverter output voltage $V_t(s)$ to grid side current $i_2(s)$ is expressed as:

$$Y(s) = \frac{i_2(s)}{V_t(s)} = \frac{1}{L_1 L_2 C_f (s+jw_g)[(s+jw_g)^2 + w_{res}^2]} \tag{2}$$

Where $w_{res} = \sqrt{\frac{L_1 + L_2}{L_1 L_2 C_f}}$ is the resonance frequency in the stationary coordinate.

When the parameter variation is considered, the state-space equations are expressed as:

$$x = \begin{bmatrix} -jw_g & \frac{1}{L_2 + \Delta L_2} & 0 \\ \frac{1}{C_f + \Delta C_f} & -jw_g & -\frac{1}{C_f + \Delta C_f} \\ 0 & -\frac{1}{L_1 + \Delta L_1} & -jw_g \end{bmatrix} x + \begin{bmatrix} 0 \\ 0 \\ \frac{1}{L_1 + \Delta L_1} \end{bmatrix} V_t + \begin{bmatrix} -\frac{1}{L_2 + \Delta L_2} \\ 0 \\ 0 \end{bmatrix} V_{pcc}$$

$$i_2 = [1 \quad 0 \quad 0]x \tag{3}$$

The transfer function from the inverter voltage to the grid side current can be calculated as

$$Y'(s) = \frac{i_2(s)}{V_t(s)} = \frac{1}{L_1' L_2' C_f' (s+jw_g)[(s+jw_g)^2 + w_{res'}^2]} \tag{4}$$

Where $L_1' = L_1 + \Delta L_1$, $C_f' = C_f + \Delta C_f$, $L_2' = L_2 + \Delta L_2$, and $w_{res'} == \sqrt{\frac{L_1' + L_2'}{L_1' L_2' C_f'}}$

The dynamic behavior of the grid side current in dq frame can be expressed as third order derivative terms :

$$\frac{d^{(3)} i_{2d}}{dt} = \frac{1}{b_0} V_{td} - w_{res}^2 \frac{di_{2d}}{dt} + f_d(i_{2d}, i_{2q}, V_{gd}, V_{gq}, w_g, \Delta L_1, \Delta C_f, \Delta L_2) \tag{5}$$

$$\frac{d^{(3)} i_{2q}}{dt} = \frac{1}{b_0} V_{tq} - w_{res}^2 \frac{di_{2q}}{dt} + f_q(i_{2d}, i_{2q}, V_{gd}, V_{gq}, w_g, \Delta L_1, \Delta C_f, \Delta L_2) \tag{6}$$

Where $b_0 = \frac{1}{L_1 L_2 C_f}$, $f_d(i_{2d}, i_{2q}, V_{gd}, V_{gq}, w_g, \Delta L_1, \Delta C_f, \Delta L_2)$ and $f_q(i_{2d}, i_{2q}, V_{gd}, V_{gq}, w_g, \Delta L_1, \Delta C_f, \Delta L_2)$ (or simply noted f_d and f_q) are described as general disturbance that includes external disturbance, i.e. V_g grid voltage change, and internal dynamics, i.e. coupling term between d-axis and q-axis, parameter variation.

The main idea of the LESO is to estimate f_d and f_q and compensate for them in real time. Once the total disturbance can be canceled, plant will be simplified into concise three order system. It should be noted that d-axis and q-axis have the same controller, therefore, in the following part, the proposed controller will be explained in d-axis.

The augmented system state can be re-formulated directly from (5) including an additional state f_d meanwhile denoting $i_2 = x_{1d}$, $\frac{dx_{1d}}{dt} = x_{2d}$, $\frac{dx_{2d}}{dt} = x_{3d}$, $f_d = x_{4d}$, The augmented model is expressed as:

$$\frac{dx_d}{dt} = A_d x_d + B_d V_{td} + E_d h_d \tag{7}$$

$$y_d = C_d x_d \tag{8}$$

Where, h_d indicates the time derivative of f_d. the matrix is represented as following:

$$x_d = \begin{bmatrix} x_{1d} \\ x_{2d} \\ x_{3d,} \\ x_{4d} \end{bmatrix}, \ A_d = \begin{bmatrix} 0 & 1 & 0 & 0 \\ 0 & 0 & 1 & 0 \\ 0 & -w_{res}^2 & 0 & 1 \\ 0 & 0 & 0 & 0 \end{bmatrix}, B_d = \begin{bmatrix} 0 \\ 0 \\ b_0 \\ 0 \end{bmatrix}$$

$$C_d = [1 \quad 0 \quad 0 \quad 0], E_d = [0 \quad 0 \quad 0 \quad 1]^T. \tag{9}$$

Based on (7) and (8), LESO of the augmented plant is constructed as follow:

$$\frac{d\tilde{x}_d}{dt} = A_d \tilde{x}_d + B_d V_{td} + L_d(y_d - C_d \tilde{x}_d) \tag{10}$$

Where L_d is the observer gain vector and denotes as:

$$L_d = [\beta_1 \quad \beta_2 \quad \beta_3 \quad \beta_4]^T \tag{11}$$

B. LESO Parameter Tuning and Stability Analysis

When subtracting (10) from (7), the error can be expressed as:

$$\frac{de_d}{dt} = (A_d - L_d C_d)e_d + E_d h_d \tag{12}$$

where $e_{id} = x_{id} - \tilde{x}_{id}$,

$$A_d - L_d C_d = \begin{bmatrix} -\beta_1 & 1 & 0 & 0 \\ -\beta_2 & 0 & 1 & 0 \\ -\beta_3 & -w_{res}^2 & 0 & 1 \\ -\beta_4 & 0 & 0 & 0 \end{bmatrix} \tag{13}$$

From (13) it is known that the state observer will be stable if the roots of the characteristic polynomial of $A_d - L_d C_d$ are all in the left half plane. As we design the observer poles are all located at $-w_0$, state observer will be inherently stable and parameters are selected as:

$$\lambda(s) = (s + w_0)^4 = s^4 + 4w_0 s^3 + 6w_0^2 s^2 + 4w_0^3 s + w_0^4$$

$$= s^4 + \beta_1 s^3 + (\beta_2 + w_{res}^2)s^2 + (\beta_1 w_{res}^2 + \beta_3)s + \beta_4 \tag{14}$$

Therefore, we have the state observer gain parameter as follows:

$$\begin{cases} \beta_1 = 4w_0, \\ \beta_2 = 6w_0^2 - w_{res}^2 \\ \beta_3 = 4w_0^3 - \beta_1 w_{res}^2 \\ \beta_4 = w_0^4 \end{cases} \tag{15}$$

C. Controller Design

According to the state feedback law in LADRC, the control signal is designed as:

$$u = \frac{k_p(r - \tilde{x}_{d1}) - k_{d1}\tilde{x}_{d2} - k_{d2}\tilde{x}_{d3} - \tilde{x}_{d4}}{b_0} \tag{16}$$

where r is the reference input, $\tilde{x}_{d1}$ to $\tilde{x}_{d4}$ are state of observer, after the observer obtain the states, these states will be send back into the controller.

The closed loop characteristic equation is given by:

$$s^3 + k_{d2}s^2 + (k_{d1} + w_{res}^2)s + kp = 0 \tag{17}$$

If the closed loop poles are place at w_c, then we have the following equation:

$$(s + w_c)^3 = s^3 + 3w_c s^2 + 3w_c^2 s + w_c^3 = 0 \tag{18}$$

By equating (17) and (18) we have the controller's parameter as equation (19)

$$\begin{cases} k_p = w_c^3 \\ k_{d1} = 3w_c^2 - w_{res}^2 \\ k_{d2} = 3w_c \end{cases} \tag{19}$$

Normally, the relationship between w_0 and w_c is $w_0 = 3 \sim 10 w_c$. In this paper we chose $w_0 = 10 w_c$.

III. FREQUENCY DOMAIN ANALYSIS OF LADRC

The LADRC state space controller, observer with LCL filters can be converted into frequency domain transfer function using Laplace transform as is shown in Fig.2
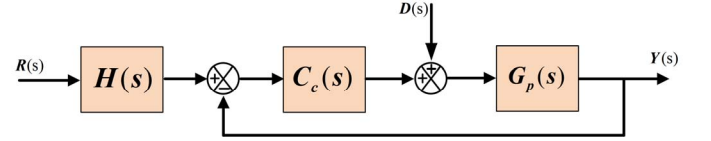

Fig. 2. Block Diagram of System of ADRC in transfer function Form

A. Loop Gain Frequency of Parameter Variation

As is shown in Fig.2. *R(s), D(s), Y(s)* are separately denoted as: reference input signal, disturbance input signal and output signals, the PWM is linearized by one order Pade approximation in $C_c(s)$. H(s) is the set point filter. Detailed derivation of the transfer function can be referred to as [11], With the parameter given in the Table I, bode plots of the open loop transfer function with parameter serious variation are shown in the following part.

Table. I: LADRC and System Parameter

LCL filter	$L_1 = 1.8\text{mH}, L_2 = 1.8\text{mH}, C_f = 27uF$
Grid inductance	$L_g = 2mH$
ESO Parameter	$\beta_1 = 0.17, \beta_2 = 8.9510e^3, \beta_3 = 2.3269e^8$ $\beta_4 = 2.3638e^{12}$
Controller Parameter	$k_p = 6.4e^{10}, k_{d1} = 6.84\text{e}^6, \ k_{d2} = 12000$
Closed loop bandwidth	$w_c = 4000\text{rad/s}$
ESO bandwidth	$w_0 = 10w_c$

First, from (2) it is known that L_1 and L_2's variation has the same effect on the loop gain frequency response after neglecting parasitic resistance, therefore, only L_1's variation will be examined. As is shown in Fig.3 and Fig.4(zoomed-in Figure) when L_1 changed from 0.9mH to 6mH while the rest of the system parameters keep nominal value, magnitude of the open-loop frequency response decreases as the inductance rise to almost 7 times of the minimal value, the cross-over frequency continues to drop as well. However, the phase margin just drops from 60 degree to 44 degree, which illustrates LADRC is quite robust to parameter L_1 variation.

Furthermore, the frequency response of filter capacitor C_f's variation is also examined as is illustrated in Fig.5 and Fig.6(zoomed-in Figure). Similar to the inductor's variation frequency response, when the capacitor value soars from $10\mu F$ to $90\ \mu F$, magnitude of the loop-gain frequency response reduce, Nevertheless, phase margin slightly drop from 57 degree to 45 degree, which also reveals the LADRC is quite immune to the capacitor's variation.
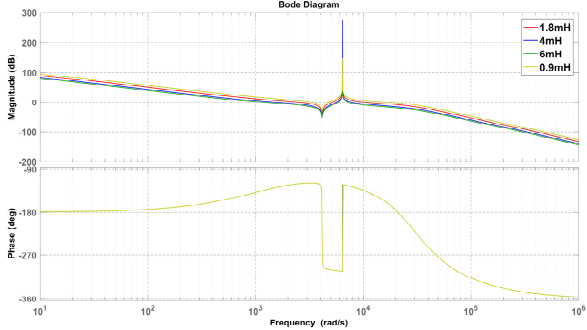

Fig. 3.   Loop Gain Bode plot for L_1 variation
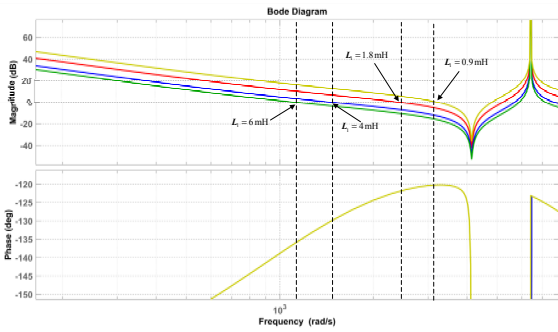
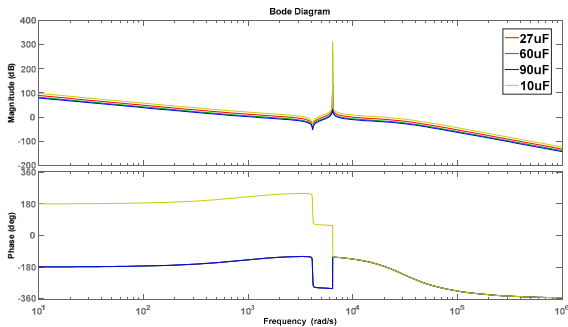Fig. 4.   Zoomed-in Bode plot for L_1 variation

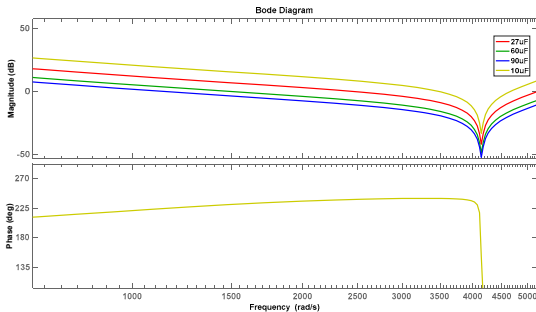Fig. 5.   Loop Gain Bode plot for C_f Variation

Fig. 6.   Zoomed-in Bode plot for C_f Variation

Inductor's parasite resistance variation is another factor that affects the precise control of inverter. Fig.7 and Fig.8(zoomed-in Figure) presents the frequency response when the total inductor's parasite resistance shifts from zero to $1.5ohm$. In the low frequency, as the value of R increases, the magnitude of the open-loop frequency response falls slightly, but the phase margin keeps almost the same. On the contrary, in the middle and high frequency section, in spite of the parasitic resistance variation, the magnitude margin, phase margin and crossover frequency are all unaffected to the parameter perturbation.
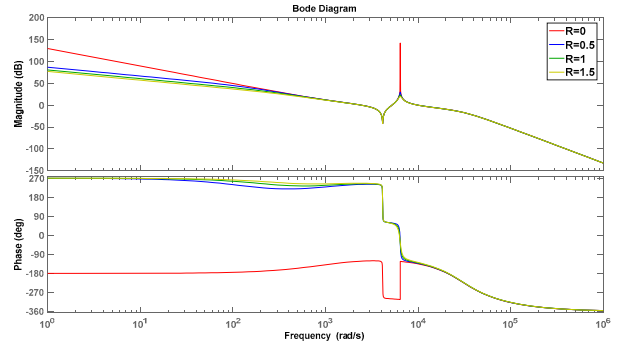

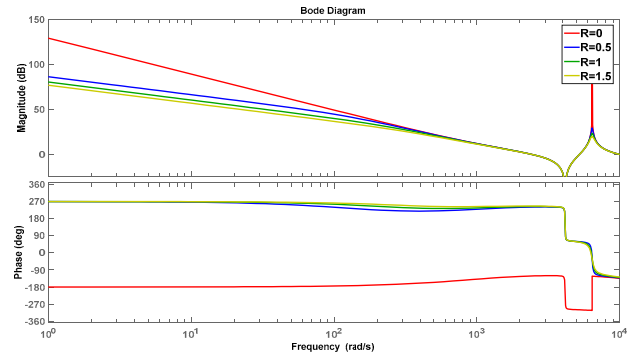Fig. 7.   Loop Gain Bode plot for parasitic resistance R variation

Fig. 8.   Zoomed-in Bode plot for R Variation

B. Disturbance Rejection

In this section, the disturbance rejection ability will be examined in terms of serious uncertainty of inductor, capacitor and inductor parasitic resistance. the bode plots of closed-loop transfer function from disturbance to output when aforementioned parameters greatly altered are illustrated from Fig.9-Fig.12. Fig.9 depicts the closed-loop bode plot from disturbance to output when the inductance varies, from which it is observed that smaller inductance leads to lower disturbance mitigation ability of LADRC. But even in the worst case($L_c = 0.9mH$), the peak magnitude still lower than -10dB. Similar to the disturbance rejection capability of inductance variation, the capacitance that seriously deviates from the nominal value does not change the disturbance mitigation capability as well as shown in Fig.10. In the worst case ($C_f = 10\mu F$), the peak magnitude is at -8dB. Inductor's parasitic resistance variation from 0 to 1.5 ohm almost does not change the disturbance rejection ability shown in Fig.11and Fig.12.

Fig. 9.   Bode plot of Disturbance Rejection for L_1 variation

Fig. 10. Bode plot of Disturbance Rejection for C_f variation

Fig. 11. Bode plot of Disturbance Rejection plot for parasitic resistance R variation

Fig. 12. Zoomed-in Disturbance Rejection for parasitic resistance R variation

IV. CASE STUDY

The effectiveness of the proposed control strategy is verified by simulation. Simulation parameter is the same as Table I.

A. Operation During Grid Disturbance

First, disturbance rejection of the proposed method under grid dips and harmonics is examined.

1) Grid-Voltage dips

Disturbance rejection against the grid-voltage dip of 0.2 p.u is evaluated. The measured voltage and current at PCC, d axis current and q axis current are respectively shown in Fig.13. As is shown from d-axis and q-axis current at 0.3s, d-axis current jump from 20 to 23A and q-axis current has 0.7A change in response to the voltage dip. the proposed method is able to reject the voltage dips effectively. From the grid current plot, the current jump can hardly be observed.
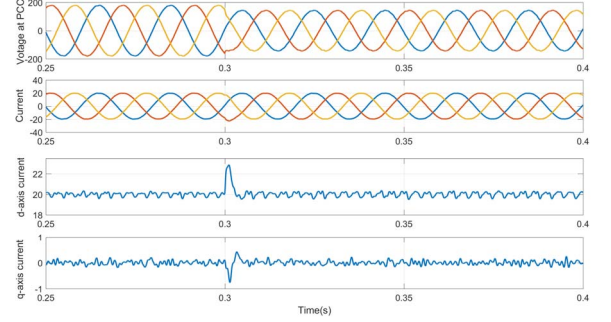

Fig. 13. Simulation Results of grid voltage, grid current, and d-axis current, q-axis current when a grid voltage dip occurs.

2) Grid Voltage Harmonic Rejection

The 5th (5%)and 7th (5%)harmonics were superimposed to the grid voltage during 0.2s and 0.4s, when the converter is operating at unity power delivery condition. The voltage and current waveforms are shown in Fig.14. Total Harmonic Distortion(THD) of current before and after harmonic voltage superimposition are compared in Fig.15. Without harmonic disturbance, THD of output current is 1.71% lower than the IEEE Std 1547 limitation of 5%. When both the fifth and 7th harmonic voltage are increased to 5%, the measured THD at PCC is 6.34%, which has reached the maximum level of IEEE recommendation. However, the current component of 5th harmonic is 2.6% and that of 7th harmonic is only 1.7%, which indicate the proposed method can effectively mitigate the harmonic voltage disturbance.

B. Operation During Current Reference Step Change

D-axis and q-axis reference current step change take place at 0.1s and 0.2s respectively. As we can see at 0.1s the d-axis current tracking responses fast and q-axis current is almost not affected by the d-axis current change. Meanwhile, the q-axis current reference step change from 0A to 10A at 0.2s does not influence on the d-axis current operation as well.
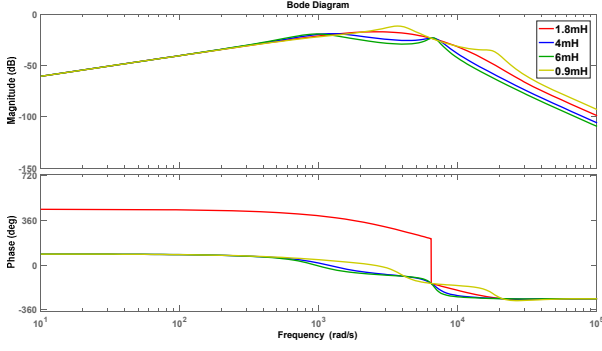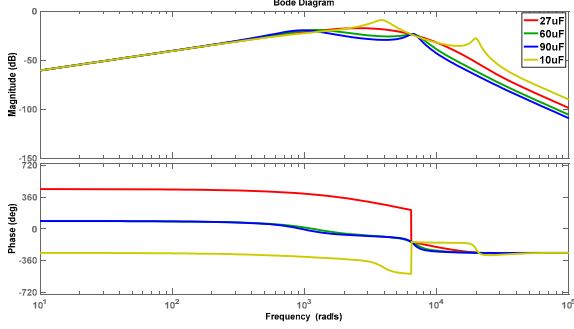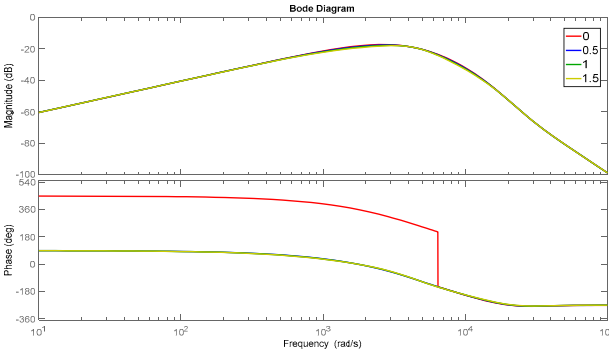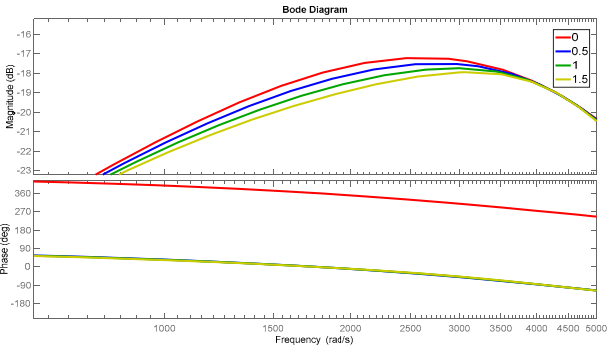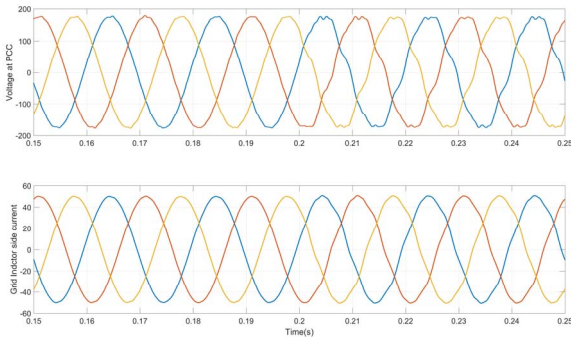
Fig. 14. Measured voltage and current when 5th and 7th harmonic superimpose on the grid voltage
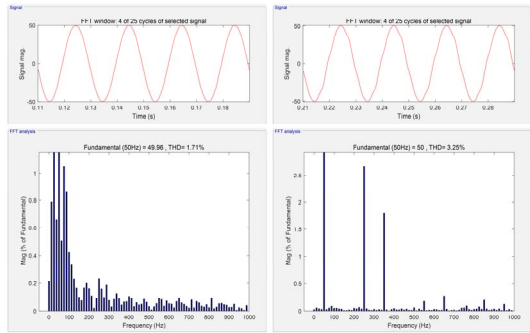

Fig. 15. THD comparison of output current before and after 5th and 7th harmonic superimpose on the grid voltage
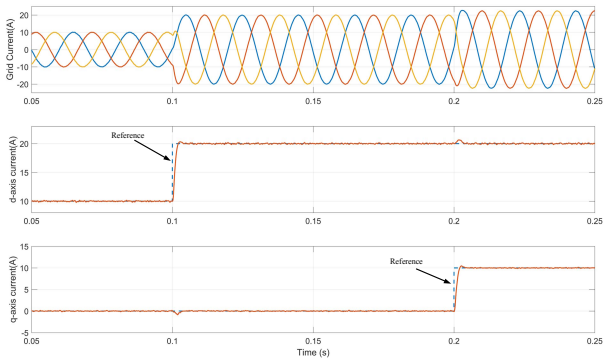

Fig. 16. Simulation Results of grid current, and d-axis current, q-axis current when d-axis current step change from 10A to 20A at 0.1s and q-axis current step change from 0A to 10A at 0.2s

V. CONCLUSION

In this paper, an LCL filter control based on LADRC was proposed. Extended state observer and controller was respectively designed based on observer bandwidth and system closed loop bandwidth The robustness of the control strategy to parameter variation and external disturbance rejection ability are examined in frequency domain. The effectiveness of disturbance rejection in LADRC was verified by simulation.

REFERENCES

[1] M. Liserre *, F. Blaabjerg, and A. Dell'Aquila, "Step-by-step design procedure for a grid-connected three-phase PWM voltage source converter," *International Journal of Electronics*, vol. 91, pp. 445-460, 2004/08/01 2004.

[2] A. A. Rockhill, M. Liserre, R. Teodorescu, and P. Rodriguez, "Grid-Filter Design for a Multimegawatt Medium-Voltage Voltage-Source Inverter," *IEEE Transactions on Industrial Electronics*, vol. 58, pp. 1205-1217, 2011.

[3] M. A. Gaafar and M. Shoyama, "Active damping for grid-connected LCL filter based on optimum controller design using injected grid current feedback only," in *Energy Conversion Congress and Exposition (ECCE), 2014 IEEE*, 2014, pp. 3628-3633.

[4] V. Miskovic, V. Blasko, T. M. Jahns, A. H. C. Smith, and C. Romenesko, "Observer-Based Active Damping of <inline-formula> <img src="/images/tex/749.gif" alt="LCL"> </inline-formula> Resonance in Grid-Connected Voltage Source Converters," *IEEE Transactions on Industry Applications*, vol. 50, pp. 3977-3985, 2014.

[5] J. Kukkola, M. Hinkkanen, and K. Zenger, "Observer-Based State-Space Current Controller for a Grid Converter Equipped With an LCL Filter: Analytical Method for Direct Discrete-Time Design," *IEEE Transactions on Industry Applications*, vol. 51, pp. 4079-4090, 2015.

[6] N. Hoffmann, M. Hempel, M. C. Harke, and F. W. Fuchs, "Observer-based grid voltage disturbance rejection for grid connected voltage source PWM converters with line side LCL filters," in *Energy Conversion Congress and Exposition (ECCE), 2012 IEEE*, 2012, pp. 69-76.

[7] K. Lee, T. M. Jahns, T. A. Lipo, V. Blasko, and R. D. Lorenz, "Observer-Based Control Methods for Combined Source-Voltage Harmonics and Unbalance Disturbances in PWM Voltage-Source Converters," *IEEE Transactions on Industry Applications*, vol. 45, pp. 2010-2021, 2009.

[8] J. Han, "From PID to Active Disturbance Rejection Control," *IEEE Transactions on Industrial Electronics*, vol. 56, pp. 900-906, 2009.

[9] G. Zhiqiang, "Scaling and bandwidth-parameterization based controller tuning," in *American Control Conference, 2003. Proceedings of the 2003*, 2003, pp. 4989-4996.

[10] O. Kiyoshi, "Realization of fine motion control based on disturbance observer," in *2008 10th IEEE International Workshop on Advanced Motion Control*, 2008, pp. 1-8.

[11] G. Tian and Z. Gao, "Frequency Response Analysis of Active Disturbance Rejection Based Control System," in *Control Applications, 2007. CCA 2007. IEEE International Conference on*, 2007, pp. 1595-1599.